

Regional distribution of sea level changes resulting from enhanced greenhouse warming in the Model for Interdisciplinary Research on Climate version 3.2

Tatsuo Suzuki¹ and Masayoshi Ishii^{1,2}

Received 30 September 2010; revised 23 November 2010; accepted 2 December 2010; published 19 January 2011.

[1] Using the Model for Interdisciplinary Research on Climate version 3.2 (MIROC 3.2), we investigated the physical nature of regional sea level changes due to enhanced greenhouse warming. The regional sea level changes were not spatially uniform, and their patterns were principally determined by the baroclinic component (density change) due to surface fluxes of heat, freshwater, and wind stress. Sea level changes in the barotropic circulation were mainly confined to the Southern Ocean. We decomposed the baroclinic response into vertical modes of ocean climatological stratification, considering the vertical structure of the baroclinic pressure change. The first baroclinic mode was responsible for about 78% of the variance in the baroclinic response, suggesting that the regional distribution of sea level change under global warming is mainly determined by displacement of the main pycnocline. The second and third modes were responsible for about 12% and 4% of the variance, respectively, some of which was related to subduction of the global warming signal. The decomposition of the baroclinic response mentioned above is suggestive of sea level changes due to global warming as results of region-by-region physical processes. **Citation:** Suzuki, T., and M. Ishii (2011), Regional distribution of sea level changes resulting from enhanced greenhouse warming in the Model for Interdisciplinary Research on Climate version 3.2, *Geophys. Res. Lett.*, 38, L02601, doi:10.1029/2010GL045693.

1. Introduction

[2] This study examined the physical nature of the regional distribution of century-scale sea level change under global warming conditions, using a coupled atmosphere-ocean general circulation model (AOGCM). Sea level changes are an important aspect of future climate change for human societies and the environment. Hence future projections of sea level change have been estimated using various AOGCMs. *Gregory et al.* [2001] compared projections based on policy-relevant scenarios for greenhouse gas emissions during the 21st century and found that changes were not spatially uniform, with some regions experiencing more than twice the global average sea level rise. Regional distributions by different models are usually not similar in detail, although there are only limited areas where the model

ensemble mean change exceeds the inter-model standard deviation [*Meehl et al.*, 2007].

[3] Some studies have suggested these sea level changes are mainly caused by sea surface wind field changes [*Landerer et al.*, 2007; *Suzuki et al.*, 2005] or combinations of wind, heat and freshwater flux changes [*Lowe and Gregory*, 2006; *Banks et al.*, 2002]. *Lowe and Gregory* [2006] also suggested that each contribution to the sea level change depends on the area. Changes in these fluxes depend on sea surface conditions such as sea level temperature, precipitation, and sea surface pressure. The geographical patterns of these changes under global warming predicted by different models show more common features, with smaller spreads among the models compared in the case of sea level changes [*Meehl et al.*, 2007]. Typically, the sea surface pressure decreases at high latitudes in both hemispheres, with compensating pressure increases over the mid-latitudes and subtropical ocean regions. This is accompanied by an expansion of the Hadley circulation and a poleward shift of mid-latitude storm tracks, which causes increased precipitation at high latitudes and decreased precipitation in the subtropics and some parts of the mid-latitudes [*Wang and Swail*, 2006; *Yin*, 2005; *Meehl et al.*, 2005]. Despite these common features, the differences in sea level changes among AOGCMs might be due to the differences in sea surface flux changes shown by the models.

[4] *Lowe and Gregory* [2006] investigated sea level changes under CO₂-induced global warming conditions in a series of idealized experiments. They used sea surface fluxes including or excluding changes in sea surface freshwater flux or wind stress under global warming conditions. They explained the causes of dynamical sea level changes in each region from these experiments. However, their results might have depended only on the one model of theirs largely, and thus they recommend similar experiments with other models to obtain more reliable future sea level projections.

[5] In this study, we used the Model for Interdisciplinary Research on Climate version 3.2 (MIROC 3.2) to understand future projection of sea level change. We conducted idealized experiments to examine the causes of regional changes, following *Lowe and Gregory* [2006]. Furthermore, we focused on the vertical pressure structure corresponding to baroclinic sea level change, to examine the physical nature of sea level change under global warming conditions.

2. Model and Experiments

[6] The model used in this study, MIROC 3.2, was developed at the Center for Climate System Research of the University of Tokyo, the National Institute for Environmental Studies, and the Frontier Research Center for Global

¹Research Institute for Global Change, Japan Agency for Marine-Earth Science and Technology, Kanagawa, Japan.

²Meteorological Research Institute, Japan Meteorological Agency, Tsukuba, Ibaraki, Japan.

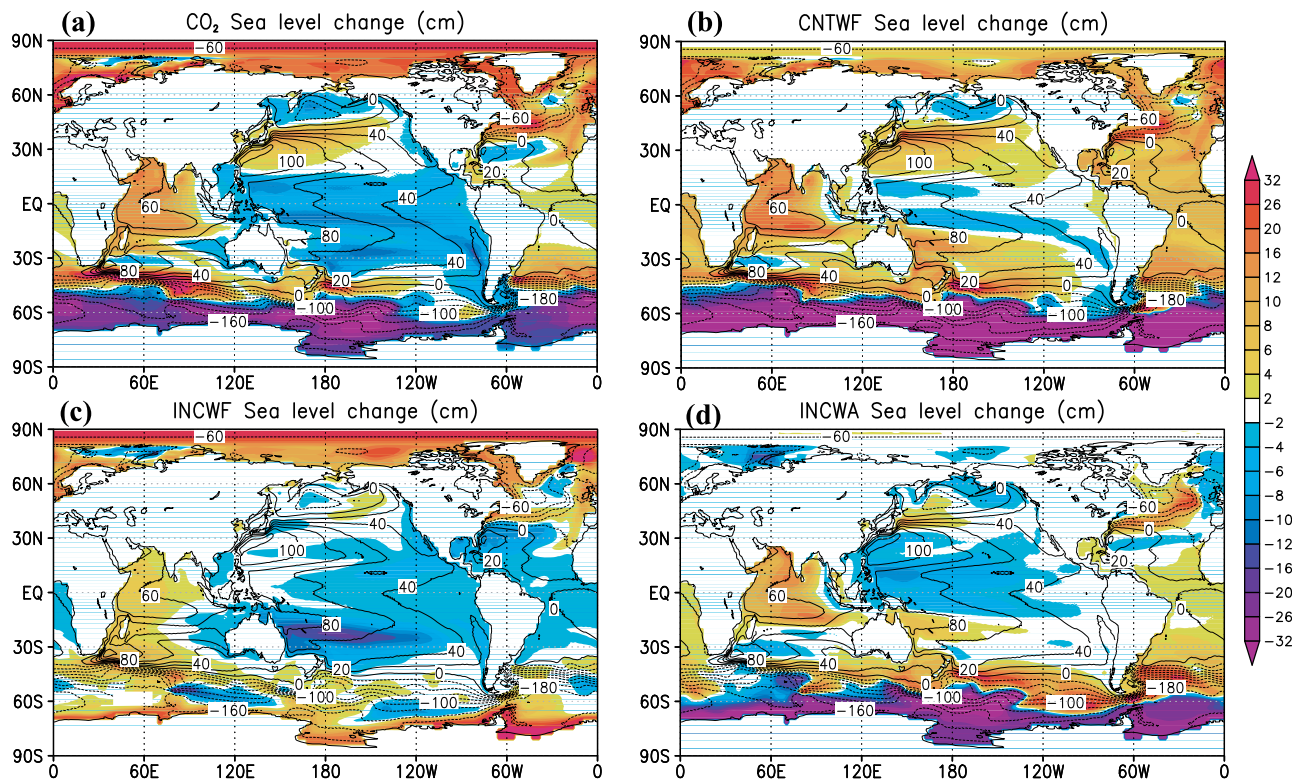


Figure 1. Sea level change from the start of the simulation to the year averaged from year 111 to year 120 (globally averaged sea level anomaly is subtracted, unit: cm): (a) CO₂ run, (b) CNTWF run, (c) INCWF run, (d) INCWA run, and sea level distribution in the control run (contour, interval: 20cm).

Change [K-1 Model Developers, 2004]. The model consists of a T42 global atmospheric spectral model with 20 vertical levels and a medium-resolution ocean model, in which the horizontal resolution is zonally 1.4° and meridionally variable (0.56° to 1.4° from the equator to high-latitudes). There are 44 vertical levels including a bottom boundary layer. The ocean component explicitly represents sea surface elevation [Killworth *et al.*, 1991], but inverted barometer effects are not applied.

[7] We spun the model up for 560 years under fixed external conditions (i.e., solar radiation, greenhouse gas concentration, aerosol emissions, and land use) for the year 1850. For a control run, we continued the integration under the same conditions for 400 years. The control run reasonably simulated annual mean climatological values and seasonal cycles of the oceanic environment corresponding to major

ocean gyres (Figure 1) [e.g., Mochizuki *et al.*, 2010; AchutaRao *et al.*, 2007; Oka *et al.*, 2006]. Tests involving CO₂-induced global warming were performed after the spin-up. In the CO₂ run, the CO₂ concentration was increased from the control value at a compound rate of 1% per year for 120 years. We performed additional idealized examinations similar to those of Lowe and Gregory [2006], in which the coupled model is integrated with modified sea surface fluxes (Table 1). Anomalous ocean surface zonal wind stress was calculated as the difference between the CO₂ run and the control run. The 10-year running mean was applied to remove interannual variation, such as the El Niño-Southern Oscillation. In the INCWA run, the CO₂ concentration was the same as in the control run, and the annual zonal wind stress anomaly from the CO₂ run was added to the atmosphere-to-ocean zonal wind stress calculated in the experiment. In the

Table 1. Experiments and Statistics on Sea Level Changes in the Last Decade^a

Experiment	Rate of CO ₂ Increase (yr ⁻¹)	Modification of Surface Flux	Spatial Standard Deviation	Area-Weighted Correlation Coefficient With CO ₂ Run ^b	Difference of Basin-Averaged Sea Level Change Between the Atlantic and the Pacific Oceans ^c
Control run	0%	None	NA	NA	NA
CO ₂ run	1%	None	11.51 cm	1.0	9.4 cm
CNTWF run	1%	Freshwater flux in control run	19.5 cm	0.76 (0.67–0.83)	7.1 cm
INCWA run	0%	Zonal wind stress anomaly	9.55 cm	0.58 (0.45–0.69)	2.9 cm
INCWF run	0%	Freshwater flux in CO ₂ run	6.3 cm	0.33 (0.16–0.48)	3.6 cm

^aNote degree of freedom (N = 120) is roughly estimated by assuming that the regional sea level changes are zonally related.

^bParenthetical values indicate 95% confidence interval by F-test.

^cAtlantic includes the Arctic Ocean and Pacific Ocean north of 30°S.

INCWF run, the daily averaged freshwater flux in the CO₂ run was used instead of the freshwater flux calculated in this experiment, and the CO₂ concentration was the same as in the control run. Finally, a CNTWF run was performed in which the daily averaged freshwater flux in the control run was applied but the CO₂ concentration was the same as in the CO₂ run. These fresh water fluxes include the effect of sea ice change. We used two procedures to modify the surface flux into the ocean: substitution of the freshwater flux and addition of anomalous zonal wind stress. The former method keeps the total freshwater flux and suppresses the effect of climate feedbacks on the substituted flux. The total freshwater flux is an important factor behind changes in the meridional overturning circulation and heat transport. Hence we applied the first method for the freshwater flux in the INCWF and CNTWF runs. However, the procedure of adding the anomalous flux did not distort shorter term variability such as the diurnal cycle. Diurnal wind mixing is important for the formation of the surface mixed layer. Therefore, we applied the second procedure for zonal wind forcing in the INCWA run. We did not add the meridional wind stress anomaly in the INCWA run explicitly. However, because of nonlinearity in the model, the meridional wind stress in the INCWA run changed with a similar pattern to that in the CO₂ run, suggesting that the effect of meridional wind change is also included in the INCWA run.

3. Regional Distribution of Sea Level Change

[8] Figure 1 shows the regional distribution of sea level change with respect to the control run for the last decade from year 111 to year 120 in the idealized anomaly experiments. To examine the regional sea level changes, we subtracted the globally averaged sea level changes in each case. The area-weighted spatial standard deviations are also given in Table 1. These values are comparable with the globally averaged sea level rise in the CO₂ run, indicating that the regional negative sea level changes act to suppress the globally averaged sea level rise, and are larger compared to the decadal variability [Suzuki *et al.*, 2005]. In the CO₂ run, the globally averaged steric sea level rise is about 29.2 cm.

[9] In the CO₂ run, positive sea level changes are seen in the Arctic Ocean, around the Kuroshio Extension (KE) and the southern recirculation of the KE, in the Indian Ocean, and along the north of the Antarctica circumpolar current (ACC). In addition, a dipole pattern of sea level changes is seen in the North Atlantic, i.e., an enhanced sea level change around 45°N and a decrease to the south. Negative sea level changes also occur around the Southern Ocean. Previous studies reported similar patterns of future sea level changes [Landerer *et al.*, 2007; Lowe and Gregory, 2006; Suzuki *et al.*, 2005]. The difference of basin-averaged sea level change between the Atlantic and the Pacific Oceans also increases (Table 1), as suggested by Landerer *et al.* [2007].

[10] In the INCWA run, the sea level changes around the KE, in the Indian Ocean and around the ACC are similar to those in the CO₂ run (Figure 1d). Wind stress changes appear to contribute to sea level changes on relatively small spatial scales compared to the scale of ocean basins. The spatial standard deviation is more than three quarters of the CO₂ run, and the area-weighted correlation coefficient with the CO₂ run is larger than that in the INCWF run (Table 1). The area-weighted correlation coefficient (Table 1) con-

firmed that adding the heat flux change improved the representation of the regional distribution of sea level change (Figures 1b and 1d). Comparing the INCWA and CNTWF runs, it is clear that heat flux change is especially important for modeling regional sea level rise in the southern recirculation of the KE and the North Atlantic. Furthermore, it enhances the sea level change around the ACC.

[11] In the CNTWF run, the regional distribution of sea level change derived by the CO₂ run is well represented; positive sea level changes around the KE and the southern recirculation, in the Indian Ocean and along the north of the ACC, and dipole pattern in the North Atlantic Ocean. However, the large positive sea level changes are not seen in the Arctic Ocean, and large negative sea level changes occur around Antarctica. Because of the large negative changes around Antarctica, the spatial standard deviation was larger than that in the CO₂ run. Lowe and Gregory [2006] suggested that changes in freshwater flux cause dipole patterns in the North Atlantic, leading to a weakening of the Atlantic meridional overturning circulation (AMOC). However, a dipole pattern is seen in the CNTWF run with a weakening of the AMOC despite the lack of freshwater flux change, suggesting that heat flux change is also an important factor for the North Atlantic dipole pattern of the CO₂ run.

[12] In the INCWF run, the positive sea level rise in the Arctic Ocean is well represented, as in the CO₂ run. Some sea level rises are shown in the Indian Ocean and around Antarctica. These results are consistent with increases of freshwater input and freshening there. Negative sea level rises are also seen in the South Pacific along 20°S. The freshwater flux change is a relatively small factor in the regional sea level changes, as demonstrated by the low spatial standard deviation and low correlation coefficient in the CO₂ run (Table 1).

4. Decomposition of Regional Sea Level Change

[13] The regional sea level change η' can be mainly decomposed into baroclinic and barotropic components in the steady state, following Lowe and Gregory [2006], Pinardi *et al.* [1995], and Fukumori *et al.* [1998]:

$$g\nabla\eta' = -\frac{g}{\rho_0 H} \int_{-H}^0 \int_z^0 \nabla\rho' dz' dz - f\mathbf{k} \times \bar{\mathbf{u}}, \quad (1)$$

where g is the gravitational acceleration, H is the depth of the ocean floor, ρ_0 is a reference density, ρ' is the density change, f is the Coriolis parameter, $\bar{\mathbf{u}}$ is the depth-averaged velocity change, and \mathbf{k} is the vertical unit vector. The first term on the right-hand side of (1) is the baroclinic component related to the density change, and the second term is the barotropic component related to the depth-averaged velocity. The baroclinic component dominates the regional sea level change, whereas the barotropic component only contributes significantly around the ACC and sub-polar gyres (Figure 2). However, the barotropic response is more important on time scales much shorter than the century-time scales discussed in this paper. These results are consistent with those of Lowe and Gregory [2006].

[14] The baroclinic pressure change depends on the vertical density structure [Gill, 1982], and the change at the sea surface is related to sea level changes. To examine the depen-

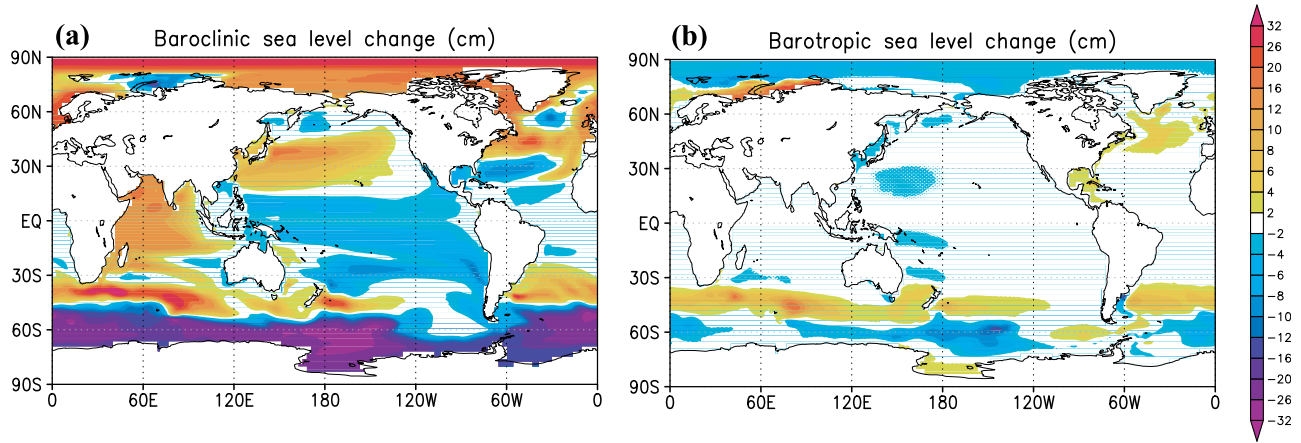


Figure 2. Sea level change from the start of the simulation to the year averaged from year 111 to year 120 in the CO₂ run (the globally averaged sea level anomaly is subtracted, unit: cm): (a) baroclinic component, (b) barotropic component.

dence of sea level change on the ocean vertical structure, the baroclinic pressure change is used as follows:

$$P'_{bc} = \rho_0 \eta'_{bc} + \int_z^0 \rho' dz', \quad (2)$$

where η'_{bc} is the baroclinic sea level change related to the first term of the right-hand side of (1). The equation is separated into a globally averaged part and its deviation:

$$P'_{bc} = \hat{P}'_{bc} + \langle P'_{bc} \rangle. \quad (3)$$

[15] The second term in this equation is related to the globally averaged steric sea level change, which is about 29.2 cm after 120-year integration in the CO₂ run. This term can be neglected when examining the pattern of regional sea level changes.

[16] From the vertically integrated (3) and (1) we obtain

$$\nabla \int_H^0 \hat{P}'_{bc} dz - \hat{P}'_{bc}(z = -H) \nabla H = 0. \quad (4)$$

[17] Assuming a flat bottom (i.e., the vertically averaged baroclinic pressure change is zero), the baroclinic pressure \hat{P}'_{bc} can be decomposed into baroclinic normal modes at each grid point

$$\hat{P}'_{bc} = \sum_{im} a_{im} P_{im}, \quad (5)$$

where a_{im} gives the contribution of each mode, and the distributions of the vertical eigenfunctions P_{im} are estimated from the model climatology in the control run. This baroclinic sea pressure change at the sea surface \hat{P}'_{bc} (Figure 3a) fully represents the regional distribution of the baroclinic sea level change (Figure 2a), suggesting that the assumption of a flat bottom is plausible. These vertical eigenfunctions include information on the vertical stratification at each point. The first mode is generally related to the main pycnocline, and the other modes also include local features of the vertical stratifications. The first baroclinic mode is responsible for about 78% of the total variance of the pressure change, the

second mode is responsible for about 12%, and the third mode is responsible for 4%.

[18] The baroclinic sea level change is well represented by the first mode, especially around the ACC and the Arctic Ocean, suggesting that these changes are related to the displacement of the main pycnocline (Figure 3b). Compared to the INCWA run (Figure 1d), these changes are almost solely responsible for the wind changes except over the Arctic Sea, where the freshwater flux change is dominant. These results suggest that the vertical displacement of the pycnocline could explain most of the regional distribution of sea level change without considering changes in the property of the water mass.

[19] The second and third modes mainly contribute at low- and mid-latitudes (Figure 3c). The vertical structures of these pressure changes have several extrema above and below the pycnocline, and the pressure changes of these modes suggest that the global warming signals are subducted into the ocean interior. This might be related to the formation of mode waters [Hanawa and Talley, 2001]. For example, such a process is often seen around the southern recirculation of the KE. A decadal oscillation accompanying subduction appeared in a 20th century hindcast by MIROC 3.2 as well [Mochizuki et al., 2010]. This regional pattern in the KE and the southern recirculation is similar to that in the CNTWF run (Figure 1c), suggesting that heat flux changes are important in this process.

[20] The fourth and higher modes represent only 6% of the total variance. Because the contributions of the higher modes to baroclinic pressure changes are generally large near the surface, composites of the fourth and higher baroclinic modes (Figure 3d) could partly explain the local water density changes near the surface in the Indian Ocean and the western tropical Pacific. Such density changes are seen in the INCWF run (i.e., the contribution of the freshwater flux change) and in the differences between the CNTWF and INCWA runs (i.e., the contribution of the heat flux change).

5. Conclusions

[21] The nature of regional sea level changes under CO₂-induced global warming conditions was investigated using MIROC 3.2 with idealized forcing experiments like those of

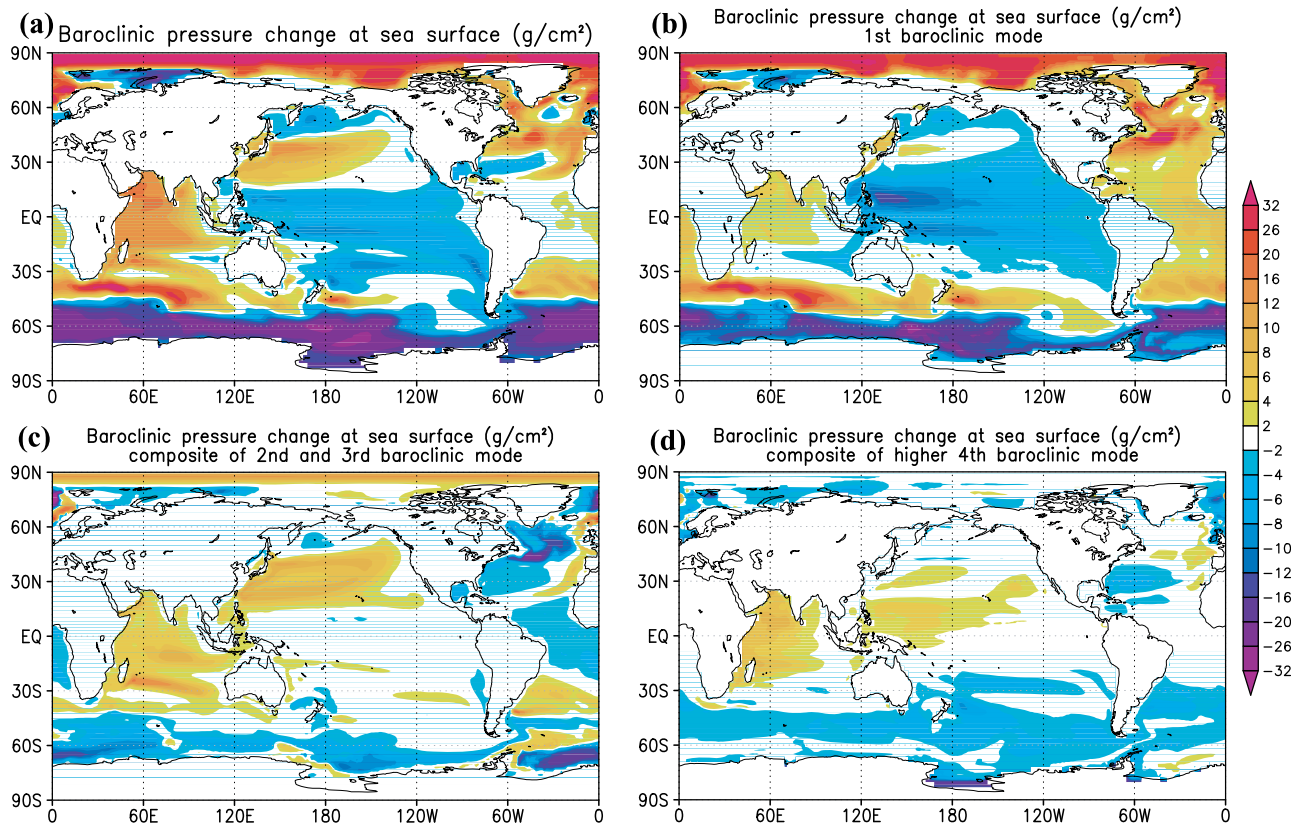


Figure 3. Baroclinic pressure change at the sea surface from the start of the simulation to the year averaged from year 111 to year 120 (unit: g/cm^2): (a) total, (b) first mode, (c) composite of second and third modes, (d) composite of the remaining modes.

Lowe and Gregory [2006]. As in previous studies, the regional distribution of sea level changes was spatially inhomogeneous and distinctively correlated to surface flux changes, with baroclinic change dominating. The baroclinic sea level changes could be decomposed into vertical modes depending on the vertical density structure. The first baroclinic mode contributed 78% of the total variance. The changes in the first baroclinic mode indicated that the vertical displacement of the pycnocline are caused by the changes in wind stress forcing, except in the Arctic Ocean, where the water mass is freshened above the pycnocline. The changes in the second and third modes implied subduction of the global warming signal, suggesting changes in the formation of mode waters. These changes were related to the heat flux changes. The contributions of higher order modes were relatively restricted near the surface, with water density changes caused by local heat or freshwater fluxes.

[22] The regional distribution of sea level changes under global warming conditions is probably caused by the vertical displacement of pycnocline by wind forcing, subduction of the warming signal and the water density change near surface. We suggest some plausible physical interpretations of each vertical mode. However, the physical processes causing local sea level changes need to be detailed more by further investigation.

[23] **Acknowledgments.** The authors thank the model developers of MIROC for discussions and helpful comments. This work was supported by the Japanese Ministry of Education, Culture, Sports, Science, and

Technology, through the Innovative Program of Climate Change Projection for the 21st Century. The numerical calculations were carried out on the Earth Simulator in the Earth Simulator Center.

References

- AchutaRao, K. M., M. Ishii, B. D. Santer, P. J. Gleckler, K. E. Taylor, T. P. Barnett, D. W. Pierce, R. J. Stouffer, and T. M. L. Wigley (2007), Simulated and observed variability in Ocean temperature and heat content, *Proc. Natl. Acad. Sci. U. S. A.*, *104*, 10,768–10,773, doi:10.1073/pnas.0611375104.
- Banks, H., R. A. Wood, and J. M. Gregory (2002), Changes to Indian Ocean subantarctic mode water in a coupled climate model as CO_2 forcing increases, *J. Phys. Oceanogr.*, *32*, 2816–2827, doi:10.1175/1520-0485(2002)032<2816:CTIOSM>2.0.CO;2.
- Fukumori, I., R. Raghunath, and L.-L. Fu (1998), Nature of global large-scale sea level variability in relation to atmospheric forcing: A modeling study, *J. Geophys. Res.*, *103*, 5493–5512, doi:10.1029/97JC02907.
- Gill, A. (1982), *Atmosphere-Ocean Dynamics*, Elsevier, New York.
- Gregory, J. M., et al. (2001), Comparison of results from several AOGCMs for global and regional sea-level change 1900–2100, *Clim. Dyn.*, *18*, 225–240, doi:10.1007/s003820100180.
- Hanawa, K., and L. D. Talley (2001), Mode waters, in *Ocean Circulation and Climate*, edited by J. Church et al., pp. 373–386, Academic, London, doi:10.1016/S0074-6142(01)80129-7.
- K-1 Model Developers (2004), K-1 coupled model (MIROC) description, edited by H. Hasumi and S. Emori, *K-1 Tech. Rep. 1*, 34 pp., Cent. for Clim. Syst. Res., Univ. of Tokyo, Tokyo.
- Killworth, P. D., D. Stainforth, D. J. Webb, and S. M. Paterson (1991), The development of a free-surface Bryan-Cox-Semtner ocean model, *J. Phys. Oceanogr.*, *21*, 1333–1348, doi:10.1175/1520-0485(1991)021<1333:TDOAFS>2.0.CO;2.
- Landerer, F. W., J. H. Jungclauss, and J. Marotzke (2007), Regional dynamic and steric sea level change in response to the IPCC-A1B Scenario, *J. Phys. Oceanogr.*, *37*, 296–312, doi:10.1175/JPO3013.1.

- Lowe, J. A., and J. M. Gregory (2006), Understanding projections of sea level rise in a Hadley Centre coupled climate model, *J. Geophys. Res.*, *111*, C11014, doi:10.1029/2005JC003421.
- Meehl, G. A., J. M. Arblaster, and C. Tebaldi (2005), Understanding future patterns of precipitation extremes in climate model simulations, *Geophys. Res. Lett.*, *32*, L18719, doi:10.1029/2005GL023680.
- Meehl, G. A., et al. (2007), Global climate projections, in *Climate Change 2007: The Physical Science Basis: Contribution of Working Group I to the Fourth Assessment Report of the Intergovernmental Panel on Climate Change*, edited by S. Solomon et al., pp. 747–845, Cambridge Univ. Press, Cambridge, U. K.
- Mochizuki, T., et al. (2010), Pacific decadal oscillation hindcasts relevant to near-term climate prediction, *Proc. Natl. Acad. Sci. U. S. A.*, *107*, 1833–1837, doi:10.1073/pnas.0906531107.
- Oka, A., H. Hasumi, N. Okada, T. T. Sakamoto, and T. Suzuki (2006), Deep convection seesaw controlled by transport through Denmark strait, *Ocean Modell.*, *15*, 157–176, doi:10.1016/j.ocemod.2006.08.004.
- Pinardi, N., A. Rosati, and R. C. Pacanowski (1995), The sea surface pressure formulation of rigid lid models: Implications for altimetric data assimilation studies, *J. Mar. Res.*, *6*, 109–119.
- Suzuki, T., H. Hasumi, T. T. Sakamoto, T. Nishimura, A. Abe-Ouchi, T. Segawa, N. Okada, A. Oka, and S. Emori (2005), Projection of future sea level and its variability in a high-resolution climate model: Ocean processes and Greenland and Antarctic ice-melt contributions, *Geophys. Res. Lett.*, *32*, L19706, doi:10.1029/2005GL023677.
- Wang, X. L., and V. R. Swail (2006), Climate change signal and uncertainty in projections of ocean wave heights, *Clim. Dyn.*, *26*, 109–126, doi:10.1007/s00382-005-0080-x.
- Yin, J. H. (2005), A consistent poleward shift of the storm tracks in simulations of 21st century climate, *Geophys. Res. Lett.*, *32*, L18701, doi:10.1029/2005GL023684.
-
- M. Ishii and T. Suzuki, Research Institute for Global Change, Japan Agency for Marine-Earth Science and Technology, Kanagawa 236-0001, Japan.